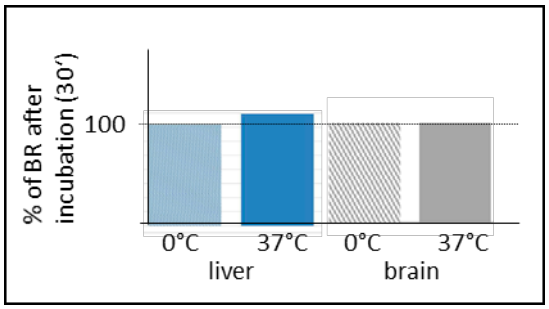

Figure S1. No loss of BR during incubation of samples subjected to the *in-vitro* HO assay with tissue homogenate. Tissue samples (liver tissue, blue; brain tissue, grey) were prepared as described for liver tissue in Material and Methods section. Samples were assembled as described for the HO assay, except that BR (30 pmol) was added instead of hemin. BR was extracted after incubating the samples on ice (0 °C, light blue, light grey) or at 37 °C (intense blue, intense grey). BR was quantified by means of spectrophotometry, as described in the Material and Methods section, and the obtained results were expressed relative to the 0 °C control determined without homogenate. Experiment was performed once.

Table S1. Information about Intron-spanning primers.

Target	Accession number	Sequence	Position on plus strand	Product-length (bp)	Exon junctions in	Intron size (bp)	Source
Cyclo	NM_008907.1	CAT GGC AAA TGC TGG ACC AAA TGC CTT CTT TCA CCT TCC CAA A	338 447	110	product	192	newly designed
HO1	NM_010442.2	CCT TCC CGA ACA TCG ACA GCC GCA GCT CCT CAA ACA GCT CAA	635 784	150	reverse primer	---	Zhao et al. (2006)
CHOP	NM_007837.4	CCC TGC CTT TCA CCT TGG CCG CTC GTT CTC CTG CTC	181 551	371	product	244	Hosoi et al. (2012)
Xbp1 (s/us)	NM_013842.3	GAA CCA GGA GTT AAG AAC ACG AGG CAA CAG TGT CAG AGT CC	720 924	205	product	771	Pfaffenbach et al. (2012)
	NM_001271739.1	GAA CCA GGA GTT AAG AAC ACG AGG CAA CAG TGT CAG AGT CC	720 898	179	product	797	
GRP78	NM_001163434.1	TCT CCA CGG CTT CCG ATA AT GTA CCT TTG TCT TCA GCT GTC ACT C	1505 1706	202	product	317	Wey et al. (2012)
IL6	NM_031168.2	GAG GAT ACC ACT CCC AAC AGA CC AAG TGC ATC ATC GTT GTT CAT ACA	187 327	141	product	1271	Guiletti et al. (2001)
HO2	NM_001136066.2	GGA CAA TGC CCA GCA ATT CA CTG CCT CCT AGT GTA CCT TTG TC	720 983	264	product reverse primer	665 ---	newly designed

Table S2. Optimised protocol and validation studies using cDNA pool (Cyclo, HO1, CHOP, Xbp1, GRP78, HO2) or amplificate (IL6) dilution series.

Target	Annealing Temp (°C)/Time (sec)	Extension Temp (°C)/Time (sec)	ΔCt (RT + to RT-)	slope	Correlation Coefficient (Pearson) R^2	Verified Dynamic Range
Cyclo	62/20	72/20	8,80	–3,463	0,997	10^5
HO1	62/20	72/20	13,76	–3,414	0,996	4^5
CHOP	62/20	72/20	16,13	–3,245	0,991	2^6
Xbp1	62/20	72/20	10,76	–3,120	0,994	4^5
GRP78	62/20	72/20	10,24	–3,216	0,998	10^5
IL6	62/20	72/20	9,04	–3,229	0,999	10^7
HO2	62/20	72/20	16,85	–3,432	1,000	4^6

ΔCq gives the lowest difference in between Cq of sample and Cq of corresponding no reverse transcriptase control measured throughout this study.

T_{melt}: melting temperature

Cyclo

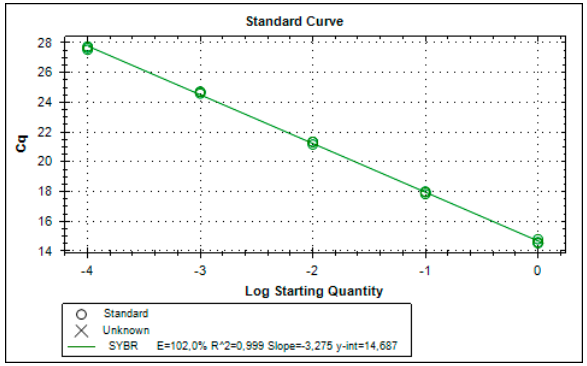

(a)

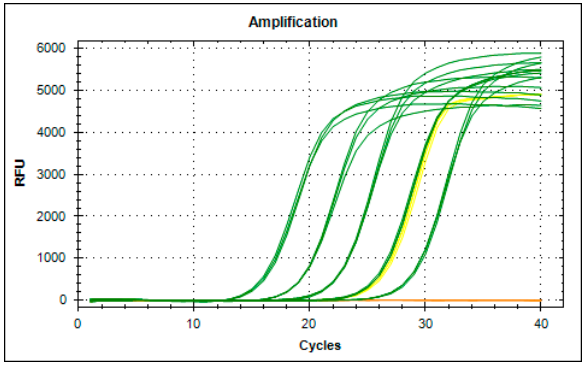

(b)

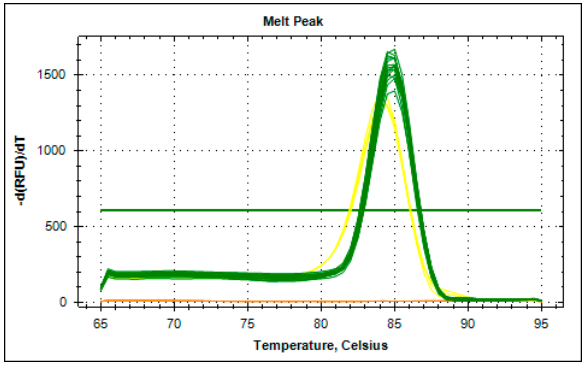

(c)

HO1

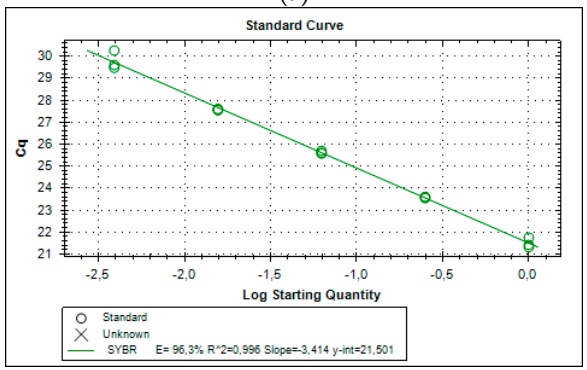

(d)

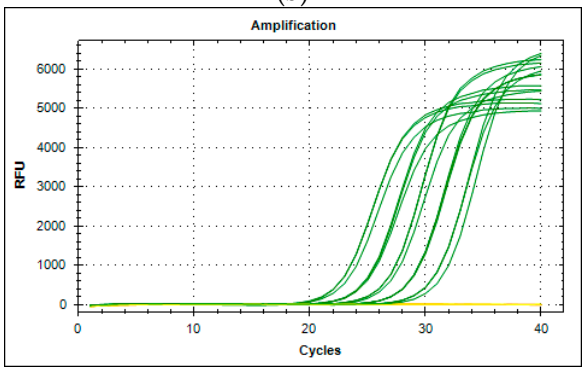

(e)

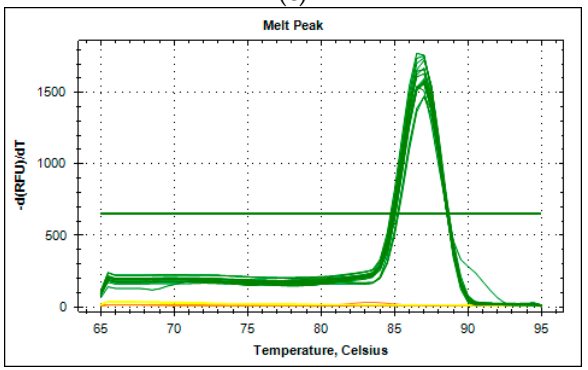

(f)

CHOP

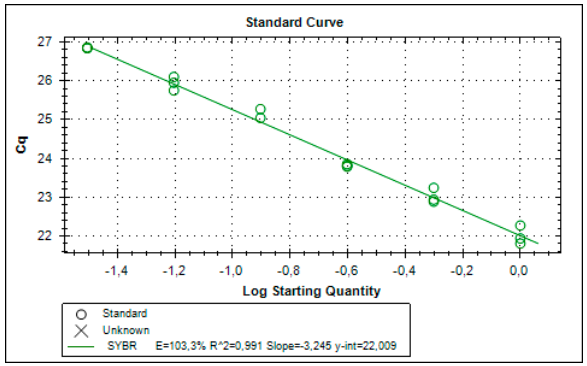

(g)

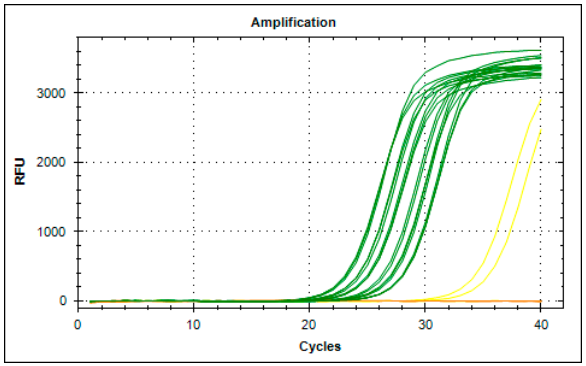

(h)

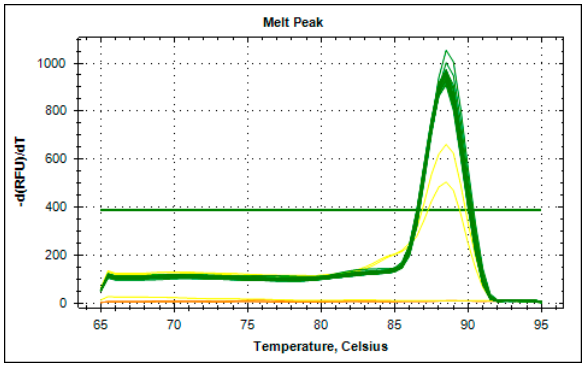

(i)

Xbp1

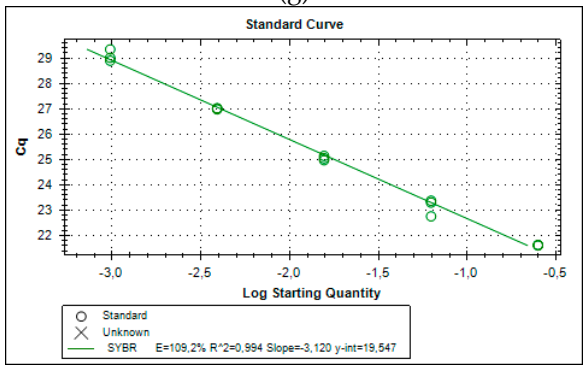

(j)

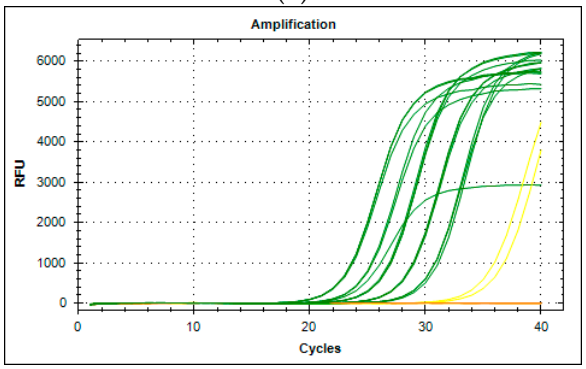

(k)

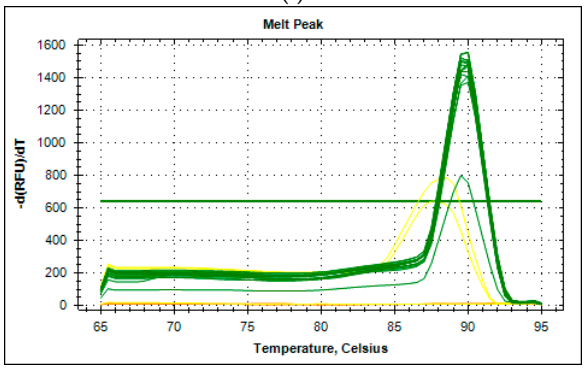

(l)

GRP78

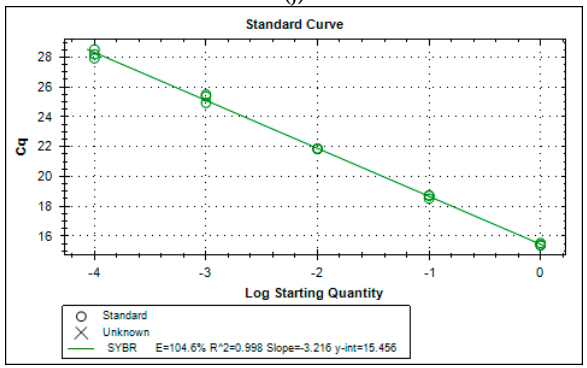

(m)

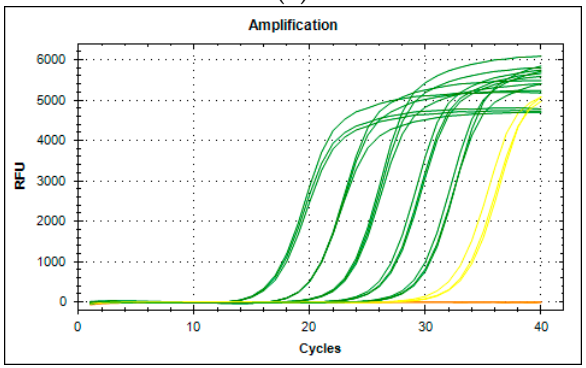

(n)

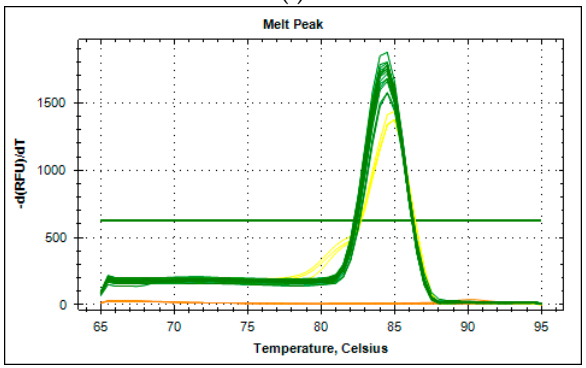

(o)

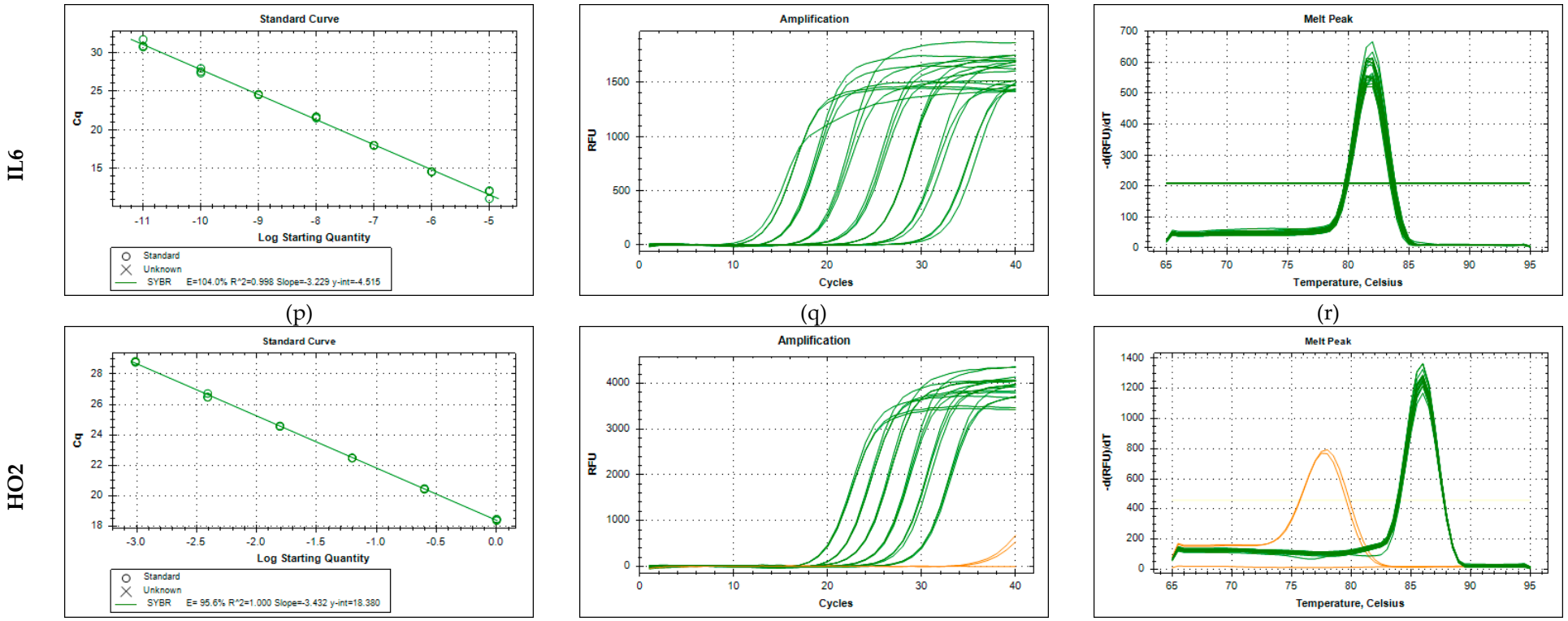

Figure S2. Performance of qPCR assays for Cyclo (**a, b, c**), HO1 (**d, e, f**), CHOP (**g, h, i**), Xbp1 (**j, k, l**), GRP78 (**m, n, o**), IL6 (**p, q, r**) and HO2 (**s, t, u**) was verified in separate experiments by performing a dilution series of a cDNA pool (**a-c, d-f, g-i, j-l, m-o, s-u)** or PCR product **(p-r**). In (**b, e, h, k, n, q, t**) amplification plots and (**c, f, i, l, o, r, u**) melt curve samples are shown in green while controls (no reverse transcription control (NRT) and no template control (NTC)) are shown in yellow and orange respectively.

Table S3. Exact p values for the data shown in figure 4.

			Neuronal Survival
§	Vehicle vs.	CBD	**0,001**
		THC	0.241
		Vehicle + Rot	**<0.001**
*	Vehicle vs.	Vehicle + BR	0.717
		Vehicle + BR +Rot	**<0.001**
#	Vehicle + Rot vs.	Vehicle + BR +Rot	0.307
		CBD + Rot	**0,002**
*	CBD vs.	CBD + BR	1.000
		CBD +BR + Rot	0.402
#	CBD + Rot vs.	CBD + BR + Rot	**0,008**
		THC + Rot	**<0.001**
*	THC vs.	THC + BR	0.07
		THC + BR + Rot	**<0.001**
#	THC + Rot vs.	THC + BR + Rot	0.807

Kruskal-Wallis test followed by Mann-Whitney-U (SPSS); signs used to display the significances are given in the first row. p<0.05 were considered significant and are highlighted in bold.

Table S4. Exact p values for the data shown in table 1.

			Metabolic Activity
*	CBD vs.	CBD + Rot	**<0.001**
		CBD + BR + Rot	**<0.001**
#	CBD + Rot vs.	CBD + BR + Rot	**0.004**
*	THC vs.	THC + Rot	**0.004**
		THC + BR + Rot	**0.019**
#	THC + Rot vs.	THC + BR + Rot	0.587

Kruskal-Wallis followed by Mann-Whitney-U (SPSS); signs used to display the significances are given in the first row. p<0.05 were considered significant and are highlighted in bold.

Table S5. Exact p values for the data shown in Figure 6.

		HO-1	HO-2	IL6	GRP78	Xbp1	CHOP
Vehicle vs.	Rotenone	1.000	1.000	1.000	1.000	1.000	**<0.001**
Vehicle vs.	CBD	**0.006**	1.000	**<0.001**	0.124	**0.007**	**<0.001**
Vehicle vs.	THC	1.000	1.000	1.000	1.000	0.330	1.000
Vehicle vs.	BR	1.000	1.000	1.000	1.000	1.000	1.000

One way ANOVA followed by Bonferroni correction (SPSS). $p < 0.05$ were considered significant and are highlighted in bold.

Table S6. Exact p values for the data shown in figure 7.

			HO-1	HO-2	IL6	GRP78	Xbp1	CHOP
§	Vehicle vs.	CBD	**0,045**	**0,025**	**<0.001**	1.000	0.128	**<0.001**
		THC	1.000	1.000	1.000	1.000	1.000	1.000
*	Vehicle vs.	Vehicle + Rot	1.000	1.000	1.000	0.348	1.000	**<0.001**
		Vehicle + BR	1.000	1.000	1.000	1.000	1.000	1.000
		Vehicle + BR + Rot	1.000	1.000	1.000	0.120	1.000	**<0.001**
#	Vehicle + Rot vs.	Vehicle + BR + Rot	1.000	1.000	1.000	1.000	1.000	1.000
*	CBD vs.	CBD + Rot	0.229	0.182	**<0.001**	**0.021**	0.126	**<0.001**
		CBD + BR	0.811	1.000	**<0.001**	1.000	1.000	**0.003**
		CBD +BR + Rot	1.000	0.168	**<0.001**	1.000	1.000	**0.014**
#	CBD + Rot vs.	CBD + BR + Rot	**0.003**	1.000	0.087	**0.037**	1.000	**<0.001**
*	THC vs.	THC + Rot	1.000	1.000	1.000	1.000	1.000	**<0.001**
		THC + BR	1.000	1.000	1.000	1.000	1.000	1.000
		THC + BR + Rot	1.000	1.000	1.000	1.000	1.000	**<0.001**
#	THC + Rot vs.	THC + BR + Rot	1.000	1.000	1.000	1.000	1.000	1.000

One way ANOVA followed by Bonferroni correction (SPSS); signs used to display the significances are given in the first row. $p<0.05$ were considered significant and are highlighted in bold.

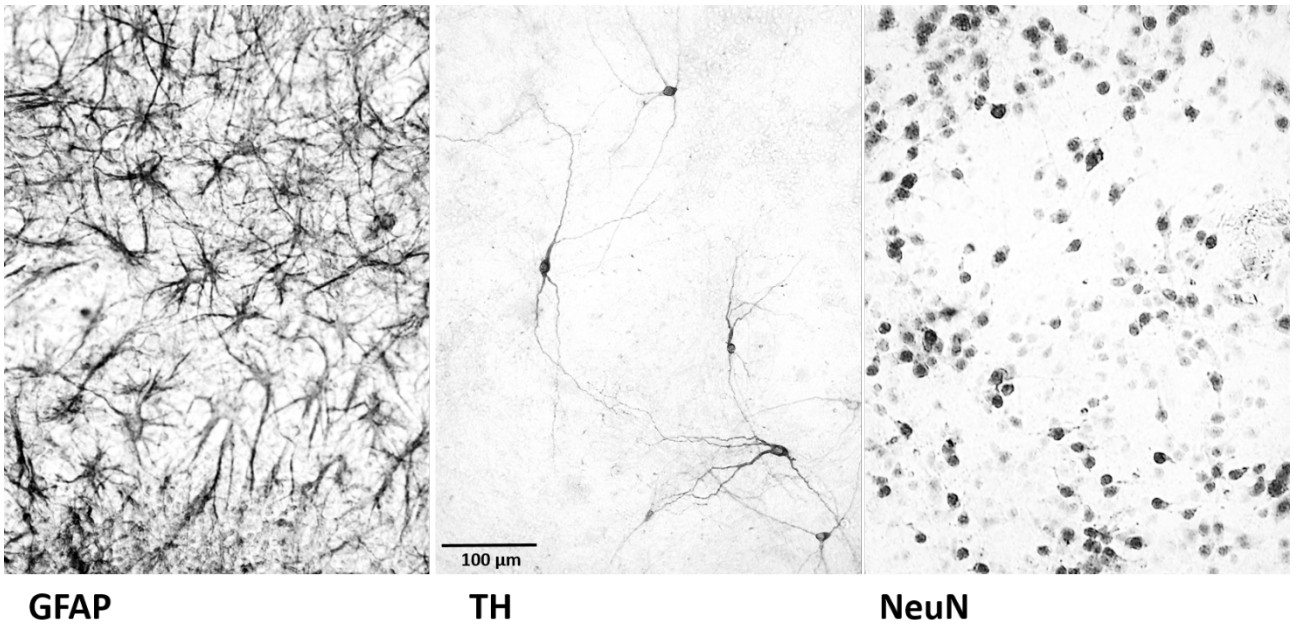

Figure S3. Immunocytostaining against glial fibrillary acidic protein (GFAP; 1:1000, Millipore, Germany), tyrosine hydroxylase (TH) and the neuronal nuclei marker NeuN (1:1000, Millipore, Germany) in mesencephalic cultures. Anti-GFAP and -NeuN staining (both 1:1000, Merck Millipore, Germany) was done according to the method described in 2.1.3. The number of dopaminergic neurons represent less than 1% of the total cell population.

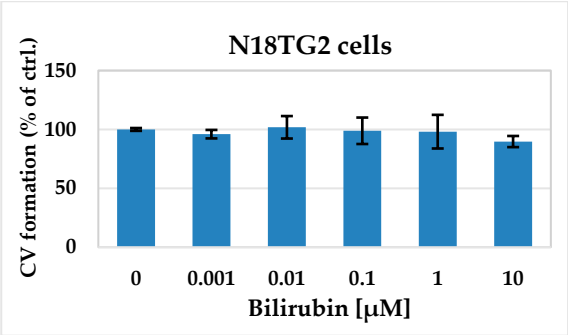

(a)

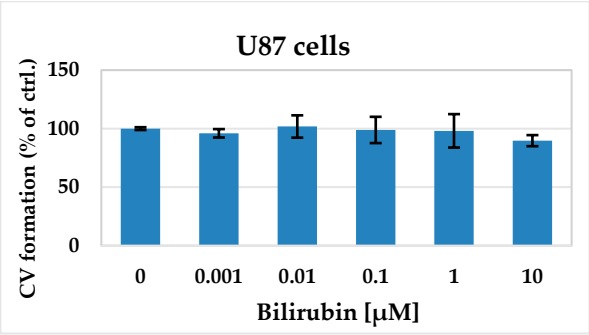

(b)

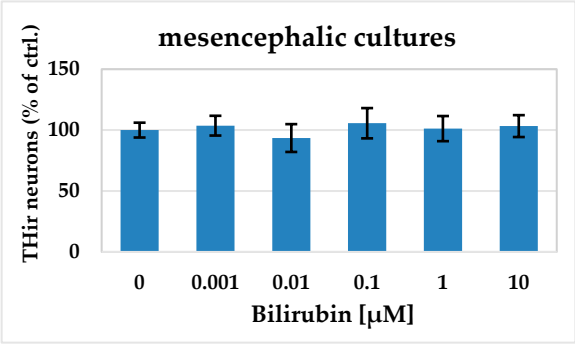

(c)

Figure S4: Effects of bilirubin on N18TG2 and U87 cells or dopaminergic neurons in primary cultures. Cells were treated with different concentrations of bilirubin (BR) for 48 h. Neuroblastoma and astrocytoma cells were stained with crystal violet (**a, b**), and dopaminergic neurons in mesencephalic primary cultures for tyrosine hydroxylase (TH, **c**) before counting. Data are shown as mean +/- SEM of four (a,b) of five (c) independent experiments, respectively. No statistical significance was detected using the Kruskal–Wallis (H) test.

Table S7. Effect of bilirubin on resazurin formation.

N18TG2 neuroblastoma cells						
BR conc. [µM]	**0**	**0.001**	**0.01**	**0.1**	**1**	**10**
mean	100	99.296	93.338	98.522	94.609	96.621
SEM	1.523	5.578	2.57	2.683	1.972	2.221

U87 astrocytoma cells						
BR conc. [µM]	**0**	**0.001**	**0.01**	**0.1**	**1**	**10**
mean	100	106.943	107.708	102.986	108.459	108.613
SEM	0.598	6.684	5.686	7.537	7.652	6.162

mesencephalic primary cells						
BR conc. [µM]	**0**	**0.001**	**0.01**	**0.1**	**1**	**10**
mean	100	99.43	100.238	97.833	97.786	95.361
SEM	2.117	3.012	3.438	2.712	2.828	3.147

In accordance to the crystal violet and tyrosine hydroxylase data, bilirubin does not affect the overall metabolism measured by the formation of resazurin. Data present the mean and the SEM of 10 (neuroblastoma cells) or 4 (astrocytoma cells and mesencephalic cultures) independent experiments, respectively. The Kruskal–Wallis (H)-test followed by the $\chi 2$-test revealed no significant difference between groups.

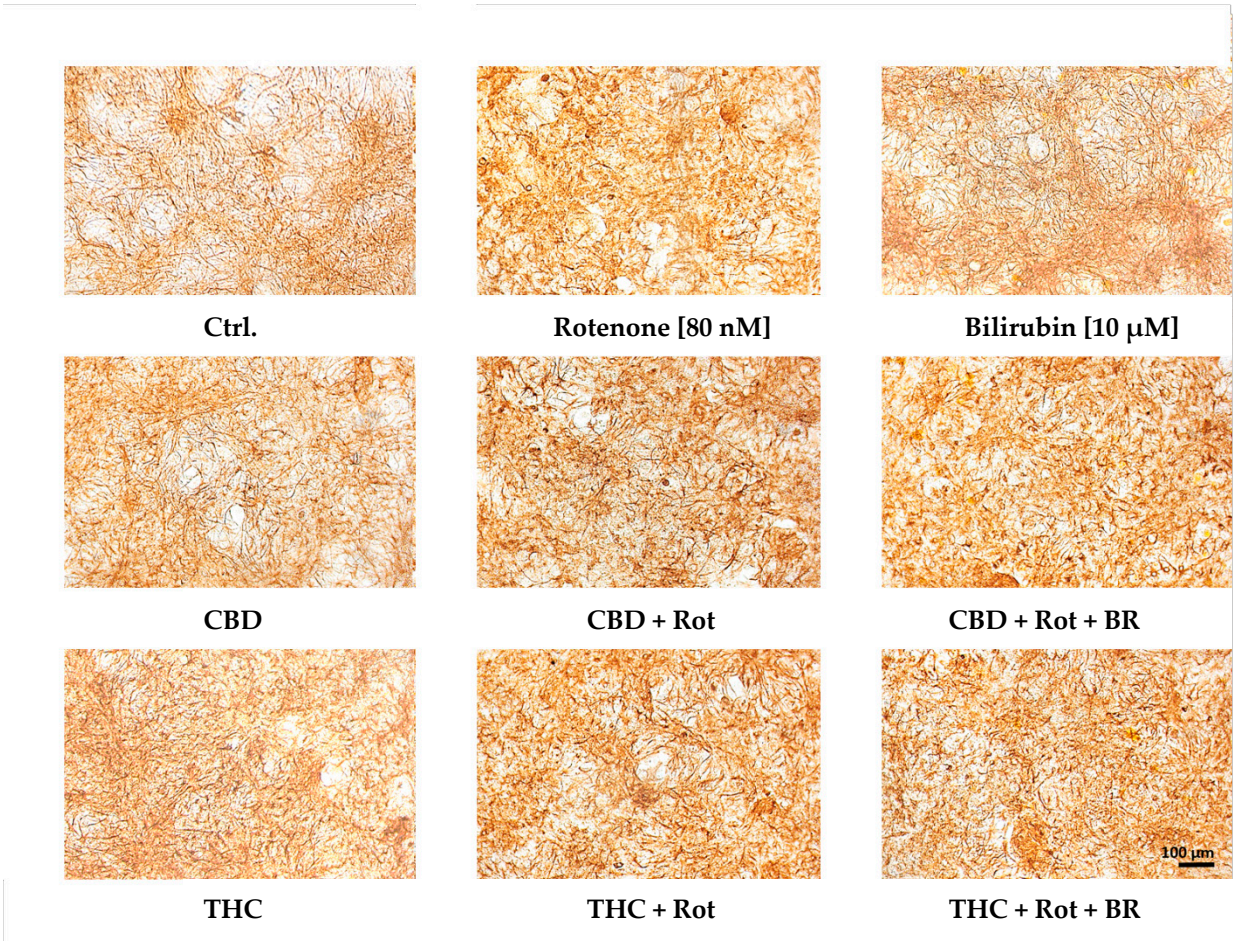

Figure S5. Glial fibrillary acidic protein (GFAP) immunocytochemistry in mesencephalic cultures. Anti-GFAP staining (both 1:1000, Merck Millipore, Germany) was done according to the method described in 2.1.3.

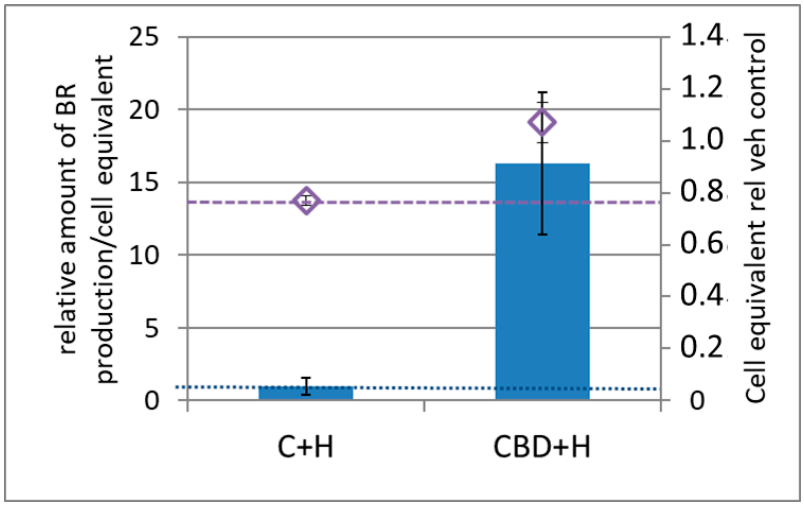

Figure S6. CBD accelerates BR formation from heme by an increased the HO reaction. N18TG2 cells were treated with heme (10µM) with or without adding CBD (10µM). The formed BR was extracted from the cell culture medium after 50 h. 150 µl of medium was supplemented with 50µl caffeine solution and 50µl KCl and the samples treated as the samples obtained in the HO-assay, as described in the Material and Methods section. Amount of BR in benzene-extracts, determined by spectrophotometry, was corrected for the underlying cell number (blue bars, primary Y-axis). Cell number was determined using the crystal violet assay and calculated as cell equivalent (violet open diamond, secondary Y-axis) given relative to the control cells, which were treated by vehicle only and set to 1 (veh control). BR extracted from the control cells was below the detection limit. Data from one experiment performed in triplicates are given as means +/- SD.